

NEUTRON CAPTURE GAMMA-RAY SPECTROSCOPY USING ^{252}Cf

A Thesis

Submitted to the Graduate Faculty of the
Louisiana State University and
Agricultural and Mechanical College
in partial fulfillment of the
requirements for the degree of
Master of Science

in

The Department of Physics and Astronomy

by

Amarakoon M. Dharmaratne Amarakoon
B.S., University of Sri Lanka, Peradeniya Campus,
Sri Lanka, 1970

December 1977

ACKNOWLEDGEMENTS

The author wishes to express his most sincere gratitude to Professor Edward F. Zganjar, whose capable direction and helpful attitude not only made this project and thesis possible, but also enjoyable. His encouragement and assistance in all aspects of my academic career throughout the course of this experiment were invaluable. Warmest thanks are offered to Dr. Ashok. Visvanathan for his valuable advice and assistance at various stages of this project and to Dr. W. Cleveland for his assistance in computer programming. The author gratefully acknowledges the guidance and the corporation given by Dr. R. C. McIlhenny, Dr. F. Iddings and Dr. J. C. Courtney of the Nuclear Science Center in the development of the experimental facility.

The financial assistance in the form of an International Atomic Energy Agency fellowship from the National Research Council, USA is gratefully acknowledged. The IAEA in Vienna, Austria and the AEA in Sri Lanka have been very helpful in making the necessary arrangements for this program of training.

TABLE OF CONTENTS

	Page
ACKNOWLEDGEMENTS	ii
LIST OF TABLES	iv
LIST OF FIGURES	v
ABSTRACT	vii
CHAPTER	
1. INTRODUCTION	1
2. EXPERIMENTAL FACILITY	2
3. THE SPECTROMETER SYSTEM	14
4. EXPERIMENTAL MEASUREMENTS	18
1. Introduction	18
2. Measurements Using a 41 μg ^{252}Cf Source	18
3. Measurements Using a 3.1 mg ^{252}Cf Source	19
4. The Capture Gamma-Ray Spectrum of Natural Hg	31
1. Energy Measurements	32
2. Intensity Measurements	35
5. EXPERIMENTAL RESULTS FROM NEUTRON CAPTURE IN NATURAL Hg	41
1. Isotopic Analysis	41
2. Decay Scheme for ^{200}Hg	51
6. DISCUSSION	54
7. CONCLUSIONS	56
LIST OF REFERENCES	57
VITA	59

LIST OF TABLES

Table		Page
1	The Energies and Abundance of Neutrons From Spontaneous Fission of ^{252}Cf	2
2	Energy Calibration Standards	34
3	Data for the Efficiency Calibration of the Detector.....	36
4	Data for the Variation of 1E/FE and 2E/FE with Full Energy.....	39
5	The Results from the $^{199}\text{Hg}(n,\gamma)^{200}\text{Hg}$ Reaction.....	42
6	The Results from the $^{201}\text{Hg}(n,\gamma)^{202}\text{Hg}$ Reaction.....	49
7	The Results from the $^{196}\text{Hg}(n,\gamma)^{197}\text{Hg}$ Reaction	50
8	The Percentage Abundance and the Thermal Neutron Capture Cross Section of ^{199}Hg , ^{201}Hg and ^{196}Hg	54

LIST OF FIGURES

Figure		Page
1	A Schematic Diagram of the Experimental Facility.....	5
2(a)	A Diagram of the Ge(Li) Detector with the $^6\text{LiCO}_3$ Filter.....	7
2(b)	A Diagram of the ^{252}Cf Source Capsule...	7
3	The Thermal Neutron Flux Curve for a 918 μg ^{252}Cf Source in Water; From Ref.6	10
4(a)	A Diagram of the ^{252}Cf Source Tube Holder.....	11
4(b)	A Diagram of the Lead Shield Configuration for the Detector.....	11
5	A Diagram of the Collimator in an Expanded Scale.....	13
6	A Block Diagram of the Spectrometer System.....	15
7	A Diagram of the Ge(Li) Crystal Illustrating the Gamma-Ray Interaction Processes.....	15
8(a)	A Diagram Indicating the Dose Rates Using a 41 μg ^{252}Cf Source.....	20
8(b)	A Diagram Indicating the Dose Rates Using a 3.1 mg ^{252}Cf Source.....	20

LIST OF FIGURES (cont'd)

	Page
9(a), (b) The Neutron Capture Gamma-Ray Spectrum From Natural Hg Using a 41 μg ^{252}Cf Source.....	21, 22
10(a), (b) The Neutron Capture Gamma-Ray Spectrum From Natural Hg Using a 3.1 mg ^{252}Cf Source.....	24, 25
11 The Background Gamma-ray Spectrum Using a 3.1 mg ^{252}Cf Source.....	26
12 The Neutron Capture Gamma-Ray Spectrum from Al Using a 3.1 mg ^{252}Cf Source.....	27
13 The Energy Calibration Spectrum.....	28
14(a), (b) The Neutron Capture Gamma-Ray Spectrum from CCl_4 Using a 3.1 mg ^{252}Cf Source	29, 30
15 The Photopeak Efficiency Curve for the Detector System.....	37
16 The 1E/FE and 2E/FE against Full Energy Curves for the Detector System	40
17 The Decay Scheme for ^{200}Hg	53

ABSTRACT

An experimental facility utilizing ^{252}Cf as a source of neutrons has been developed for neutron-capture gamma-ray spectroscopy. The applicability of the facility to nuclear energy level studies and isotopic analysis investigations has been demonstrated through a detailed study of the neutron-capture gamma-ray spectrum from a sample of natural mercury.

CHAPTER 1

INTRODUCTION

Neutron capture gamma-ray studies using sources containing ^{252}Cf have been reported by Greenwood¹ and Wiggins et al.² In the work of Greenwood¹ gamma-ray spectra of copper and basalt containing the elements aluminum, silicon, sodium, potassium, calcium, titanium, iron and magnesium were studied. In the work of Wiggins et al.² gamma-ray spectra of manganese, iron, nickel and copper were investigated. The results of both these experiments were found to be in agreement with nuclear reactor based results indicating the potential of ^{252}Cf as a source of neutrons for neutron capture gamma-ray spectroscopy.

The motivation underlying the work reported here was the development of a facility for neutron capture gamma-ray spectroscopy using ^{252}Cf and to explore the feasibility of applying the data obtained with such a facility in the construction of nuclear energy level schemes and in isotopic analysis procedures.

CHAPTER 2

THE EXPERIMENTAL FACILITY

According to the information provided in the Du Pont Report,³ the process that gives rise to the emission of neutrons from ^{252}Cf is spontaneous fission. The spontaneous fission half life of ^{252}Cf is 85.5 yrs. The yield of neutrons is 2.4×10^{12} neutrons per second from one gram. Table 1 lists the energies and the abundance of neutrons from spontaneous fission of ^{252}Cf . The specific activity of ^{252}Cf is 5.37×10^2 Ci/g.

Table 1

Energy (MeV)	n/sec g
0-0.5	2.8×10^{11}
0.5-1.0	3.7×10^{11}
1.0-2.0	7.6×10^{11}
2.0-3.0	4.6×10^{11}
3.0-4.0	2.8×10^{11}
4.0-5.0	1.6×10^{11}
5.0-6.0	5.6×10^{10}
6.0-7.0	4.0×10^{10}
7.0-8.0	1.3×10^{10}
8.0-10.0	9.9×10^9
10.0-13.0	2.2×10^9

In addition to the neutrons, the fission process of ^{252}Cf gives rise to the emission of 1.3×10^{13} gamma-rays per second from one gram. The energies of these gamma-rays extend to 6.5 MeV.

From Table 1 it is clear that the neutron energies fall within a wide range. The maximum number of neutrons is found in the energy range of 1.0 to 2.0 MeV, and the fraction of slow neutrons which are the ones useful in the work is low, less than 2.8×10^{11} n/sec g, compared to the total yield of 2.4×10^{12} n/sec g. The term "slow neutrons" is used here to include thermal neutrons and neutrons having energies up to about 1 keV. These are the ones more appropriate for (n,γ) studies because with neutrons of energies greater than about 1 keV particle reactions such as $(n,2n)$, (n,n') , (n,p) dominate⁵ over the (n,γ) reaction. Also it is clear because of the wide range of energy, the extraction of a group of neutrons having a particular energy is difficult. Because of these factors and the high output of neutrons and gamma-rays it was realized that in the construction of the experimental facility emphasis has to be placed on the following:

- a) Thermalization of ^{252}Cf neutrons and positioning of the source so as to achieve the maximum thermal flux at the target.

- b) Detector shielding from neutrons and background gamma radiation which includes gamma-rays from ^{252}Cf and from the (n,γ) reactions taking place in the materials used in the construction of the facility.
- c) Proper collimation of the gamma-rays from the target with minimal contribution from background radiation.
- d) Biological shielding from neutrons and gamma-rays.

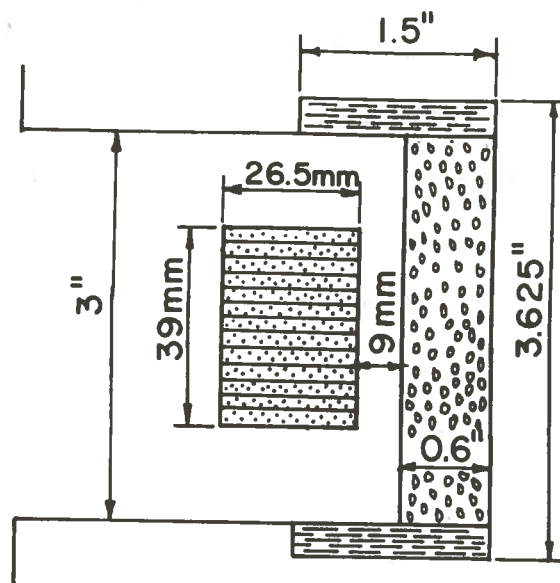
The work of Greenwood¹ has mainly been concerned with the design considerations for an experimental facility. He performed a series of measurements using a 2 mg ^{252}Cf source to optimize the design geometry, and very careful attention was given to the above aspects in designing the facility. Hence, in the construction of the experimental facility developed in this work, a number of ideas were taken from the work of Greenwood.¹

The experimental facility constructed is shown in Figure 1. The sources of ^{252}Cf were obtained from the ERDA ^{252}Cf Demonstration Facility located in the Nuclear Science Center at LSU. The ^{252}Cf was in a stainless steel capsule having the geometrical configuration shown in Figure 2(b).

The facility consisted of two concentric tanks. The outer one was made of steel and the inner one aluminum. The aluminum tank contained distilled water for

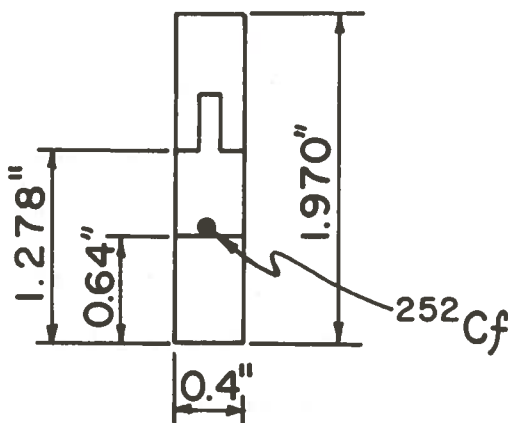
thermalization of neutrons and for slow neutron shielding. Thermalization is brought about through the scattering of neutrons off hydrogen nuclei, essentially n-p scattering. The shielding is provided through the reaction ${}^1\text{H}(n,\gamma){}^2\text{H}$ with the gamma-ray emitted having an energy of 2.22 MeV. The thermal neutron capture cross-section for hydrogen is 0.33 b^3 . Distilled water was preferred because the foreign matter, especially chlorine which has a cross-section of 43 b^4 for the reaction ${}^{35}\text{Cl}(n,\gamma){}^{36}\text{Cl}$, dissolved in ordinary water could make a significant gamma-ray contribution to the background radiation. The lead cylinder located inside the aluminum tank was to attenuate the primary gamma-rays from fission of ${}^{252}\text{Cf}$ and the capture gamma-rays from the materials in the immediate neighborhood of the source.

The space between the two tanks contained a saturated solution of boric acid. The boric acid concentration was 3 mg of B per c.c. of solution, that is 600 mg of ${}^{10}\text{B}$ per litre of solution. The isotope ${}^{10}\text{B}$ has a thermal neutron capture cross-section of 3840 b^3 for the reaction ${}^{10}\text{B}(n,\alpha){}^7\text{Li}$ accompanied by a gamma-ray of energy 0.48 MeV from the excited ${}^7\text{Li}$ nuclide. This solution was used to attenuate neutrons escaping from the water shield. Further attenuation of neutrons and gamma-rays was provided by a concrete wall which was constructed around the outer tank. The concrete wall was used only in the latter part of the experiment



DETAIL NO. 4

Figure 2(a). A Diagram of the Ge(Li) Detector with the ${}^6\text{LiCO}_3$ Filter



DETAIL NO. 5

Figure 2(b). A Diagram of the ${}^{252}\text{Cf}$ Source Capsule

as will be made clear later (Chapter 4).

The acrylic tubing through the tanks supported the collimator in one half and three WEP (Water Extendible Polyester) rods in the other half. Acrylic was chosen, because it was recognized that a material which would not intensify the background gamma radiation has to be used for this work. The chemical elements of acrylic are carbon, oxygen and hydrogen. The cross-sections for the (n, γ) reaction in carbon is 3.4 mb^4 and in oxygen it is 0.178 mb^4 . Hence acrylic appeared suitable for the work. The WEP rods were used to serve as a shield for neutrons which were scattered off the target away from the collimator. WEP is a polyester resin whose chemical elements are carbon, oxygen and hydrogen. The first two WEP rods were made by adding 500 cm^3 of water to 500 cm^3 of WEP and 10 cm^3 of 35% hydrogen peroxide which acted as a catalyst. The other WEP rod was made by adding 600 cm^3 of saturated boric acid solution to 500 cm^3 of WEP and 11 cm^3 of 35% hydrogen peroxide. Boron was added to this latter one in order to attenuate the neutrons which penetrated the other rods.

The hydrogenous moderator thickness between the positions of the source and the target was 0.8 inch. This consisted of 0.625 inch of water and 0.175 inch of acrylic. The work of Greenwood¹ and also the work at the Fort Worth Division of General Dynamics Corporation⁶

indicate that, this is the appropriate moderator thickness to achieve the maximum thermal flux at the target.

Figure 3 shows the thermal flux distribution in water based on the work performed at FWDGDC.⁶

The lead shield shown in Figures 1 and 4(b) was used to prevent background gamma-rays from reaching the detector. The configuration rested on an aluminum stand which was capable of vertical adjustment. The borated polyethylene plug shown in Figures 1 and 5 and the ${}^6\text{LiCO}_3$ filter shown in Figures 1 and 2(a) were used to prevent neutrons from reaching the detector. These neutrons are mainly those which are scattered off the target. The neutrons cause radiation damage in the Ge(Li) detector and capture of neutrons in germanium can produce background gamma-rays. This radiation damage can severely limit the useful lifetime of a Ge(Li) detector. The ${}^6\text{LiCO}_3$ filter was prepared by adding 24.5 g of this compound to a mixture containing 32 cm³ of EPON 815 and 8 cm³ of EPOXY 52 polyester resins. The carbonate was prepared by dissolving 20 g of ${}^6\text{Li}$ in a fairly concentrated solution of hydrochloric acid and treating the chloride solution with a saturated solution of sodium carbonate. The isotope ${}^6\text{Li}$ has a capture cross-section of 945 b³ for the reaction ${}^6\text{Li}(n,\alpha){}^3\text{H}$. The advantage is that no capture gamma-rays are produced as a result of the capture. This is very important, otherwise these gamma-rays would swamp the less intense flux of

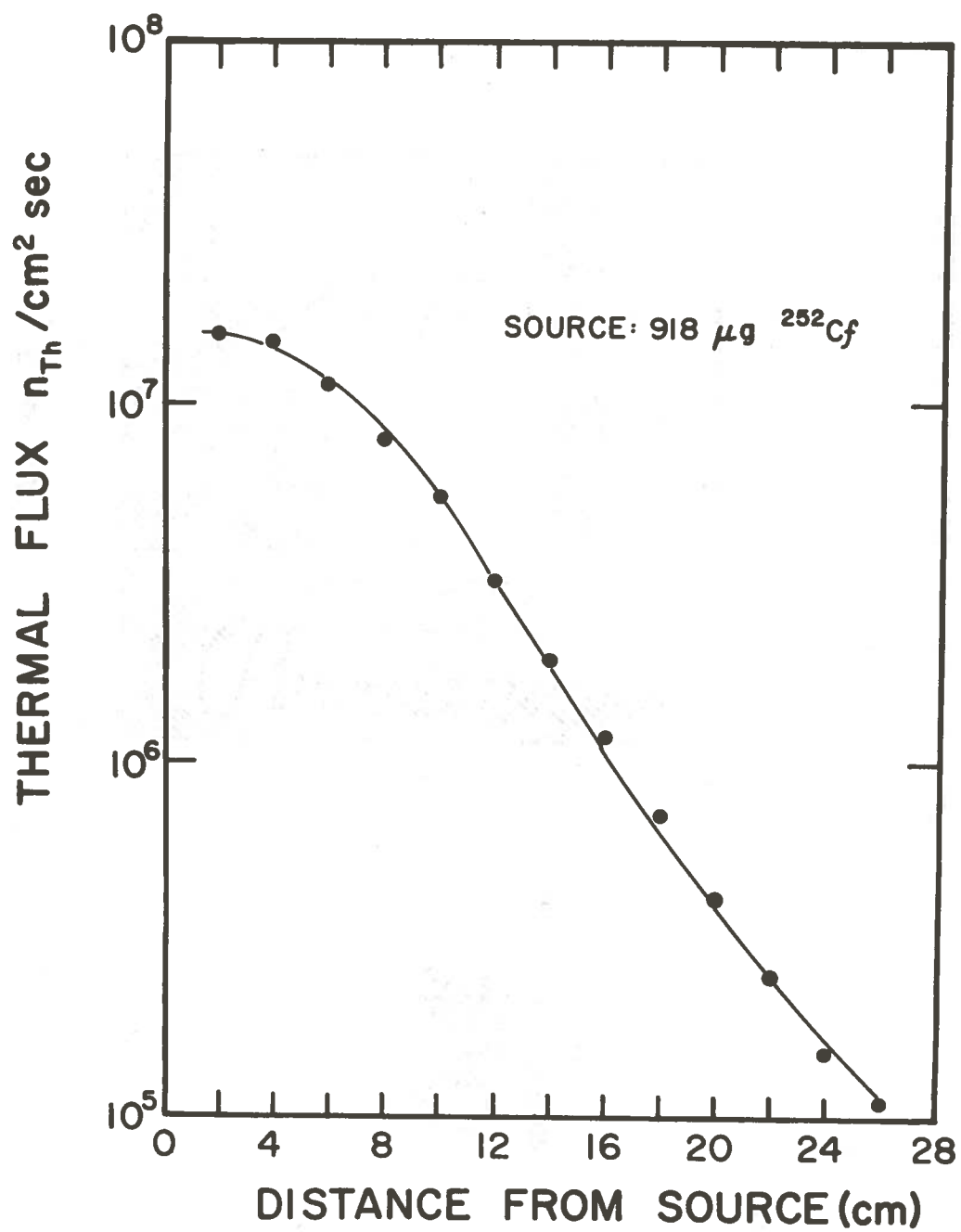


Figure 3. The Thermal Neutron Flux Curve for a 918 μg ^{252}Cf Source in Water; From Ref. 6

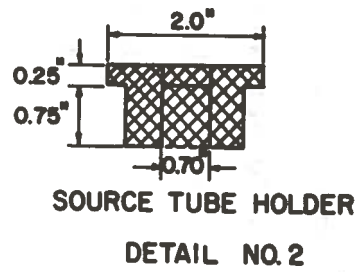


Figure 4(a). A Diagram of the ^{252}Cf Source Tube Holder

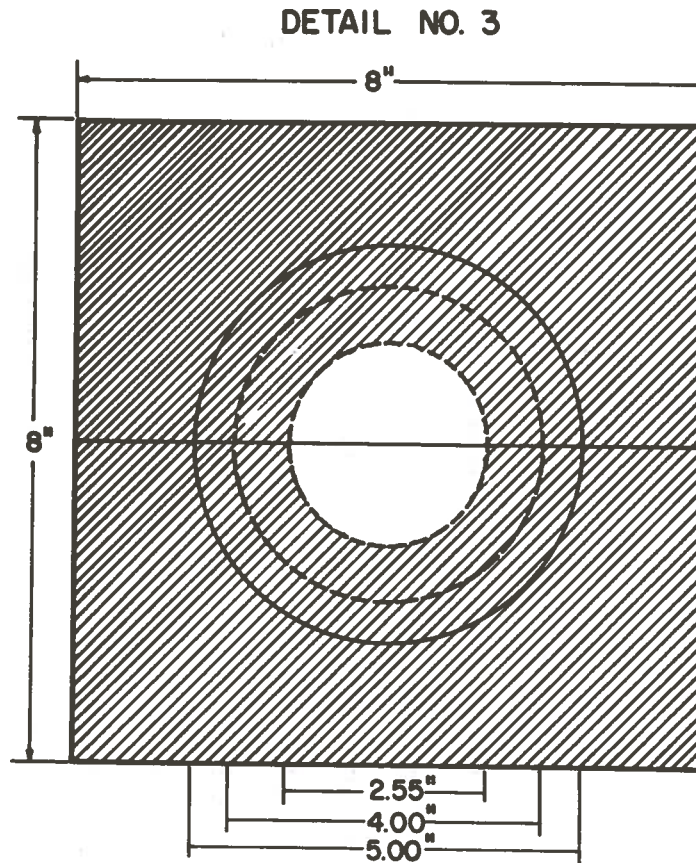


Figure 4(b). A Diagram of the Lead Shield Configuration for the Detector

gamma-rays from the target.

The collimator is shown in an expanded scale in Figure 5. The construction was based on the design of the collimator used by Greenwood.¹ The target-end of the collimator would be in a high neutron as well as gamma environment. Hence this end must consist of a material having a low neutron capture cross-section and a high Z value, to minimize the background radiation. Investigations of Greenwood¹ have revealed that bismuth was the only suitable material. Bismuth has a low neutron capture cross-section of 33mb^4 , yet it has a Z of 83. The alternate cylinders of borated polyethylene were used to attenuate neutrons penetrating the collimator material. The detector end of the collimator consisted of lead to provide attenuation of background gamma-rays. The bismuth and lead cylinders were made by melting the materials in plaster of paris molds in a He atmosphere. The melting was accomplished with the use of an induction heater. The process was performed in a He atmosphere to prevent oxidation of the materials.

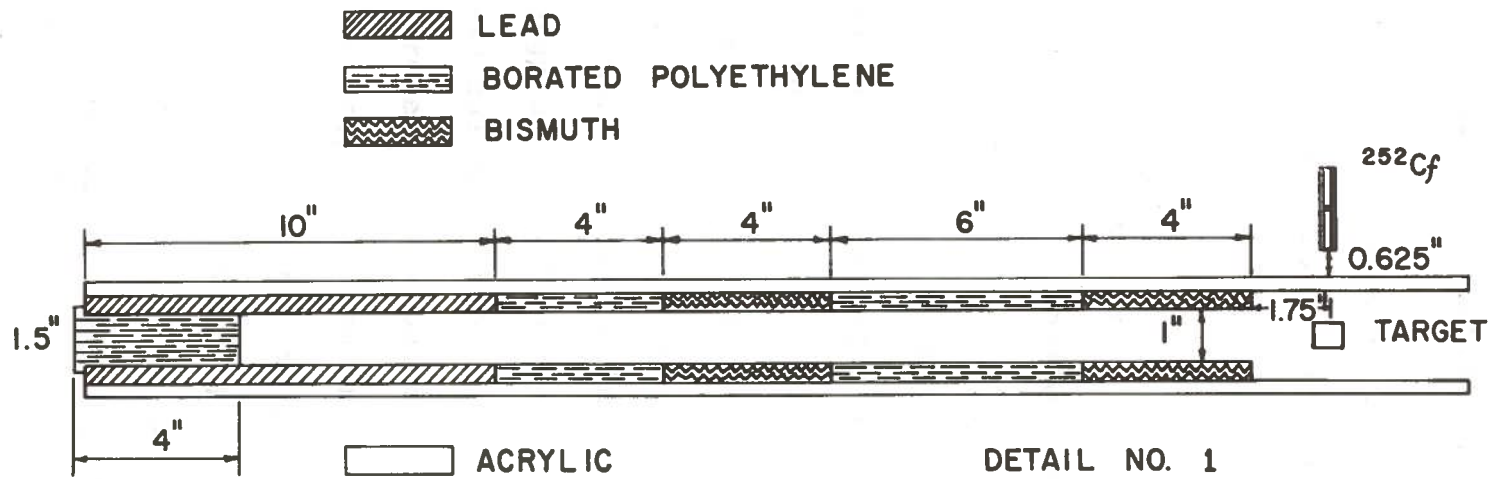


Figure 5. A Diagram of the Collimator in an Expanded Scale

CHAPTER 3

THE SPECTROMETER SYSTEM

The spectrometer system used in this experiment is shown in Figure 6. It consisted of a Ge(Li) detector coupled to a low-noise charge-sensitive preamplifier and a shaping main amplifier which in turn was coupled to a 4096 channel pulse height analyzer.

The Ge(Li) detector is a semiconductor device, basically a reverse biased p-i-n diode,^{7,8} in which ionizing radiation loses energy in producing electron-hole pairs. A gamma-ray entering a Ge(Li) detector loses its energy producing an energetic electron through the photoelectric effect, Compton effect, or pair production process. These processes are shown in Figure 7. The electron produced moves under the influence of the applied field losing energy by impact ionization creating electron-hole pairs. These charge carriers are collected at the appropriate electrodes and the pulse of charge is proportional to the energy deposited in the detector by the gamma-ray. The pair production has a threshold energy equal to the combined electron and positron rest mass energy of 1.022 MeV.² The positron is unstable and it annihilates with an electron producing two gamma-rays, each of energy 0.511 MeV.² One or both of these gamma-rays can escape the detector without further interaction and

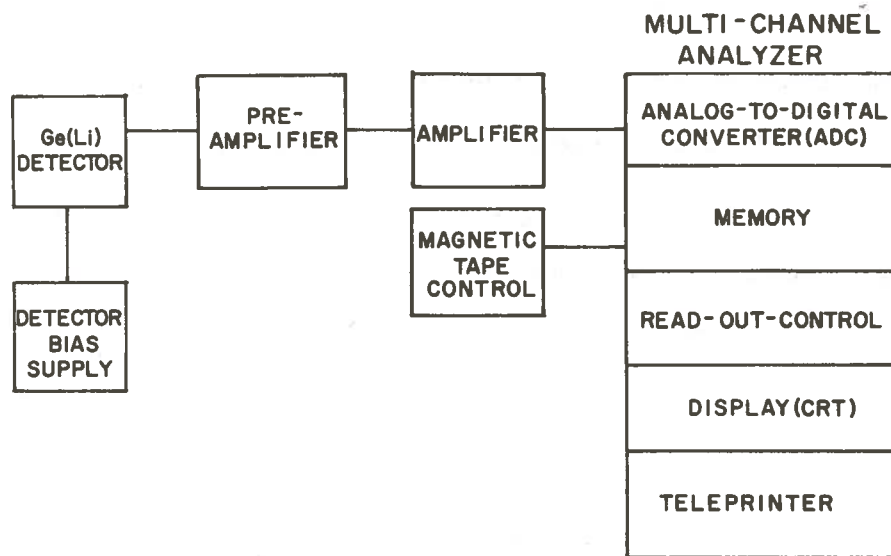


Figure 6. A Block Diagram of the Spectrometer System

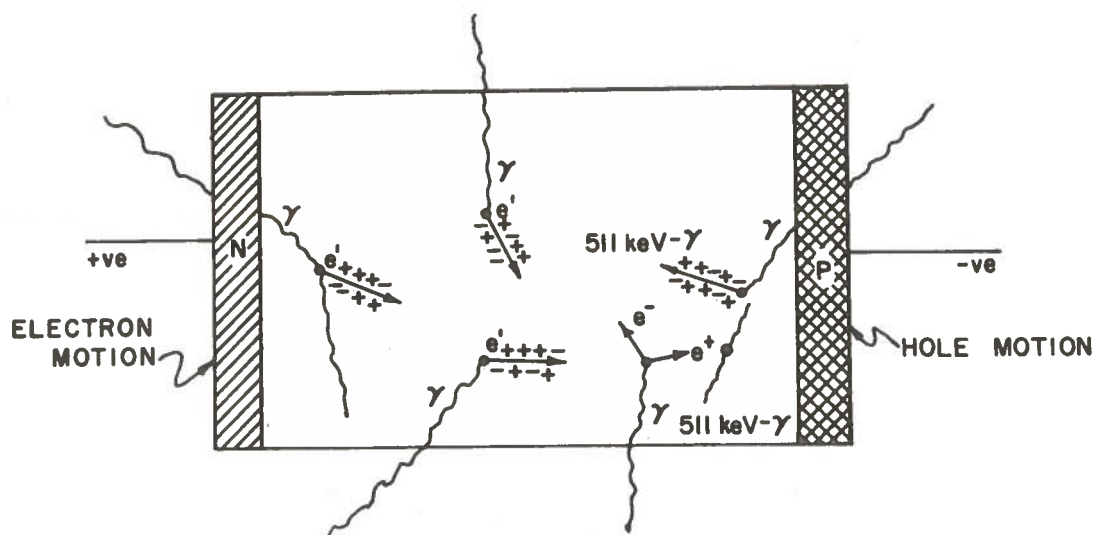


Figure 7. A Diagram of the Ge(Li) Crystal Illustrating the Gamma-Ray Interaction Processes

in the gamma-ray spectrum three peaks are observable for gamma-rays of energy greater than 1.022 MeV. These correspond to the energies E_γ , $E_\gamma - 0.511$ and $E_\gamma - 1.022$ MeV and are known as the full energy peak, the single escape peak and the double escape peak, respectively.

The signals from the detector consist of short pulses of electrical charge collected between the detector electrodes. The preamplifier senses these pulses of charge created by the incident radiation in the detector, converts them to voltage pulses,^{7,8} then amplifies and makes them suitable for transmission to the main amplifier.

The main amplifier provides additional gain to the voltage pulses from the preamplifier and provides for shaping of the pulses.^{7,8} Also, it shortens the time duration of the pulses to reduce the probability of pulse pile up which occurs when two or more pulses are closely spaced in time.

After ionizing events in the detector are converted to voltage pulses by the preamplifier and are amplified and shaped by the main amplifier, the pulses are sorted according to their pulse height and stored in the memory section of the multichannel analyzer.^{7,8} The pulse height analysis is accomplished by means of an analog-to-digital converter (ADC). A pulse entering the ADC triggers a circuit, called the voltage ramp generator or simply the

ramp, which begins to increase in voltage while a clock-pulse generator simultaneously starts producing digital pulses at a rate of 50 megahertz. When the voltage level of the ramp matches the voltage of the pulse, the pulse height has been converted to the time needed for the ramp and pulse to become equal. This time is represented by the number of signals from the pulse generator. The digital pulses cause a register, called the address scaler to advance by an amount equal to the number of pulses in the digital pulse train. This amount represents the channel (location in the ferrite core memory) in which the event is registered.

The Ge(Li) detector used in this experiment was a Canberra model 7229, operated at a bias of 2500 volts. The observed energy resolutions (FWHM) were 4.8 keV, 5.0 keV and 8.9 keV at energies 367.9 keV 2223.3 keV and 5660.1 keV, respectively. The energy resolution of the detector is the measure of the ability to resolve two gamma-rays having nearly equal energies and is usually expressed as Full Width at Half Maximum (FWHM) of the photopeaks.

The preamplifier used was the Canberra model 1408 C. The main amplifier was the Ortec model 440 and the ADC was Nuclear Data model 510 capable of digitizing up to 12 bits (4096 channels).

CHAPTER 4
EXPERIMENTAL MEASUREMENTS

4.1 Introduction

Natural mercury in the form of the stable oxide (HgO), carbon tetrachloride (CCl₄) and aluminum (Al) were used as targets in these experiments. The emphasis was placed on the study of the gamma-ray spectrum from mercury because natural mercury consists of seven stable isotopes, the gamma-ray transitions in mercury isotopes are known^{12,13,14,15} and hence the potential of the facility toward isotopic analysis and energy level study can conveniently be tested. The gamma-rays from carbon tetrachloride were used in the efficiency calibration of the detector and the gamma-rays from aluminum were used in the energy determination of the mercury lines.

4.2 Measurements Using a 41 μg ²⁵²Cf Source

To obtain an idea of the radiation level outside the facility and to examine the detection sensitivity, it was decided to first use a 41 μg ²⁵²Cf source with a neutron output of 9.8×10^7 n/sec. The only shielding required for this source was provided by lead, distilled water and the boric acid solution. The dose rates observed at different locations outside the facility are indicated in Figure (8a).

The maximum dose rate observed was 1.5 mrem/hr, which was well below the permissible personal exposure of 2.5 mrem/hr.³ This indicated that a stronger source could be used in the facility with additional shielding around the tank. The detection sensitivity was examined by observing the gamma-ray spectrum from a sample of mercury. The thermal flux estimated at the position of target, assuming a flux of 5×10^7 n/cm² sec for a 2 mg ²⁵²Cf source,¹ was 1.0×10^6 n/cm² sec. A sample of 8.54 g of HgO having a purity of 99% was irradiated for 17 hours. The spectrum obtained is shown in Figures 9(a) and (b). The presence of mercury lines was observed in this spectrum which indicated that the sensitivity was adequate and that the goal of the experiment could easily be accomplished using a stronger source.

4.3 Measurements Using a 3.1 mg ²⁵²Cf Source

A 3.1 mg ²⁵²Cf source was used in the facility to obtain the necessary data. The neutron output of this source was 7.4×10^9 n/sec and the thermal flux estimated at the position of the target was 7.7×10^7 n/cm² sec. Additional shielding for this source was provided with 20 inches of concrete. The thickness of concrete needed was estimated on the basis of the information provided in the Du Pont Report.⁹ The estimated dose rate outside the concrete wall using this

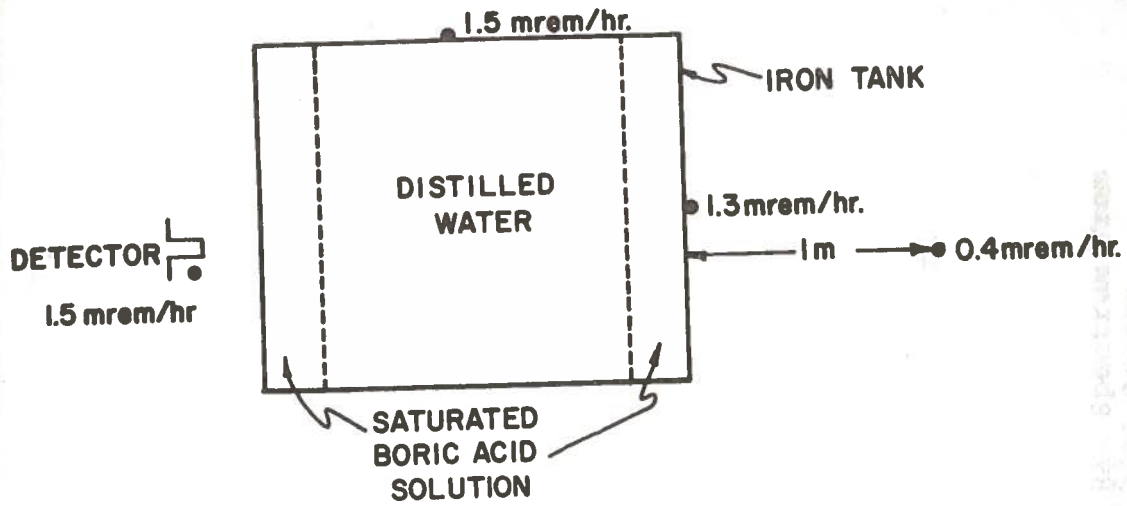


Figure 8(a). A Diagram Indicating the Dose Rates Using a $41 \mu\text{g } ^{252}\text{Cf}$ Source

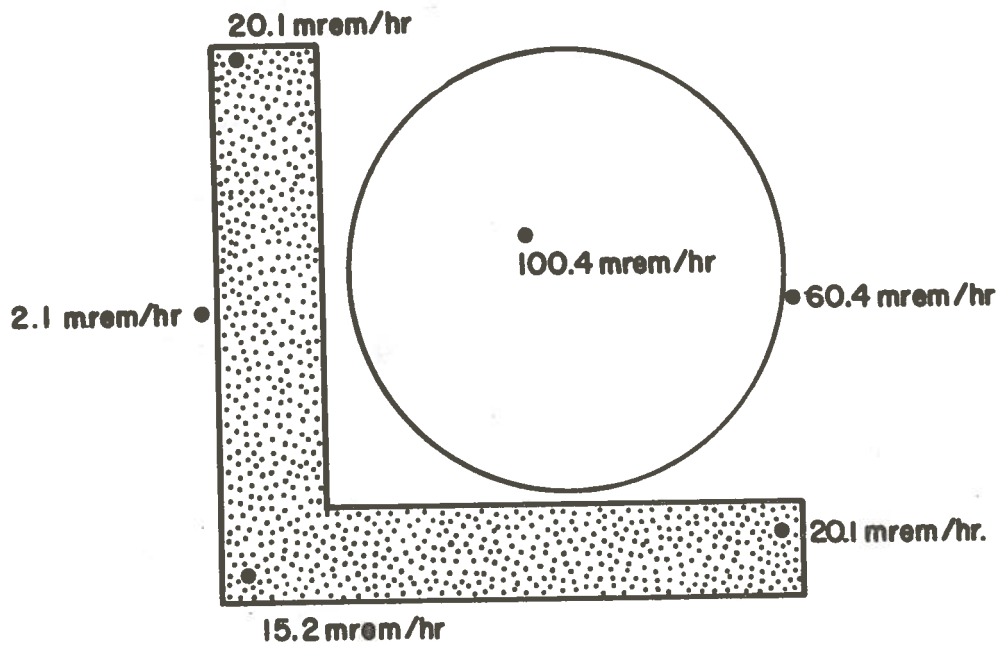


Figure 8(b). A Diagram Indicating the Dose Rates Using a $3.1 \text{ mg } ^{252}\text{Cf}$ Source

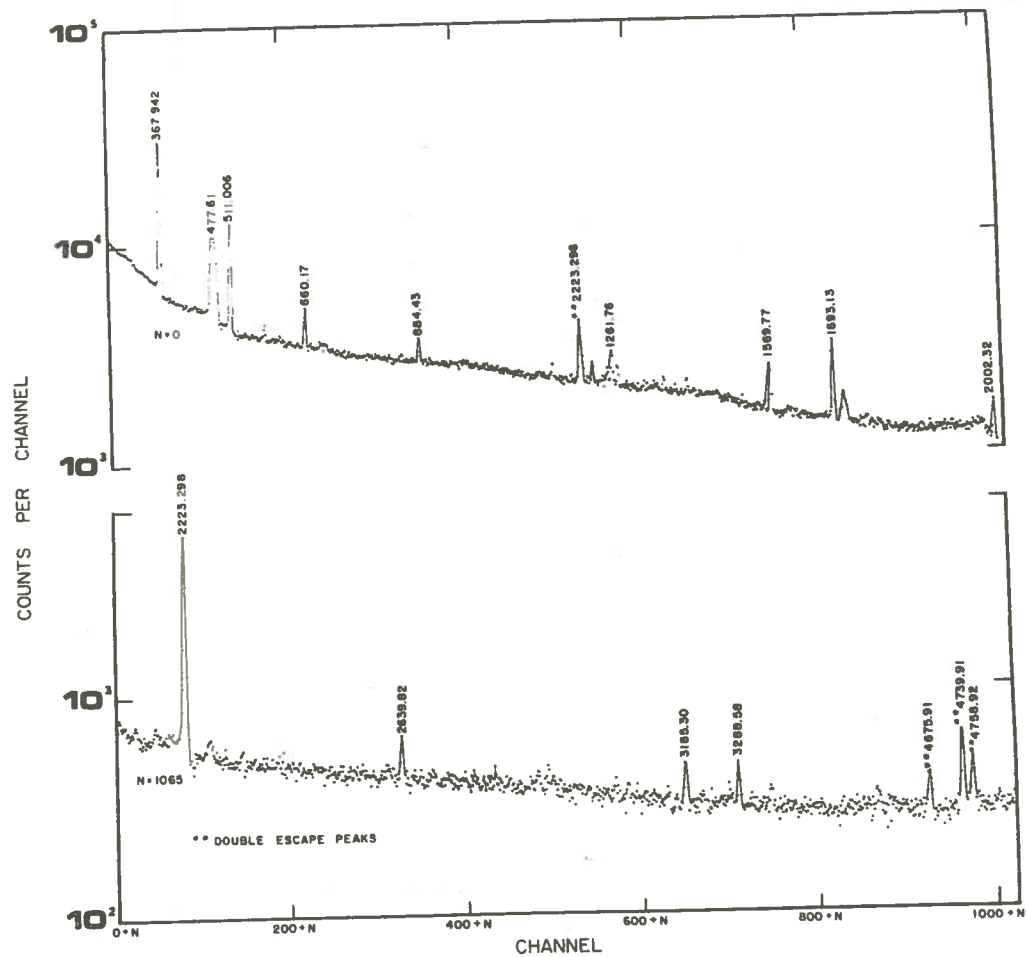


Figure 9(a). The Neutron Capture Gamma-Ray Spectrum From Natural Hg Using a $41 \mu\text{g}$ ^{252}Cf Source

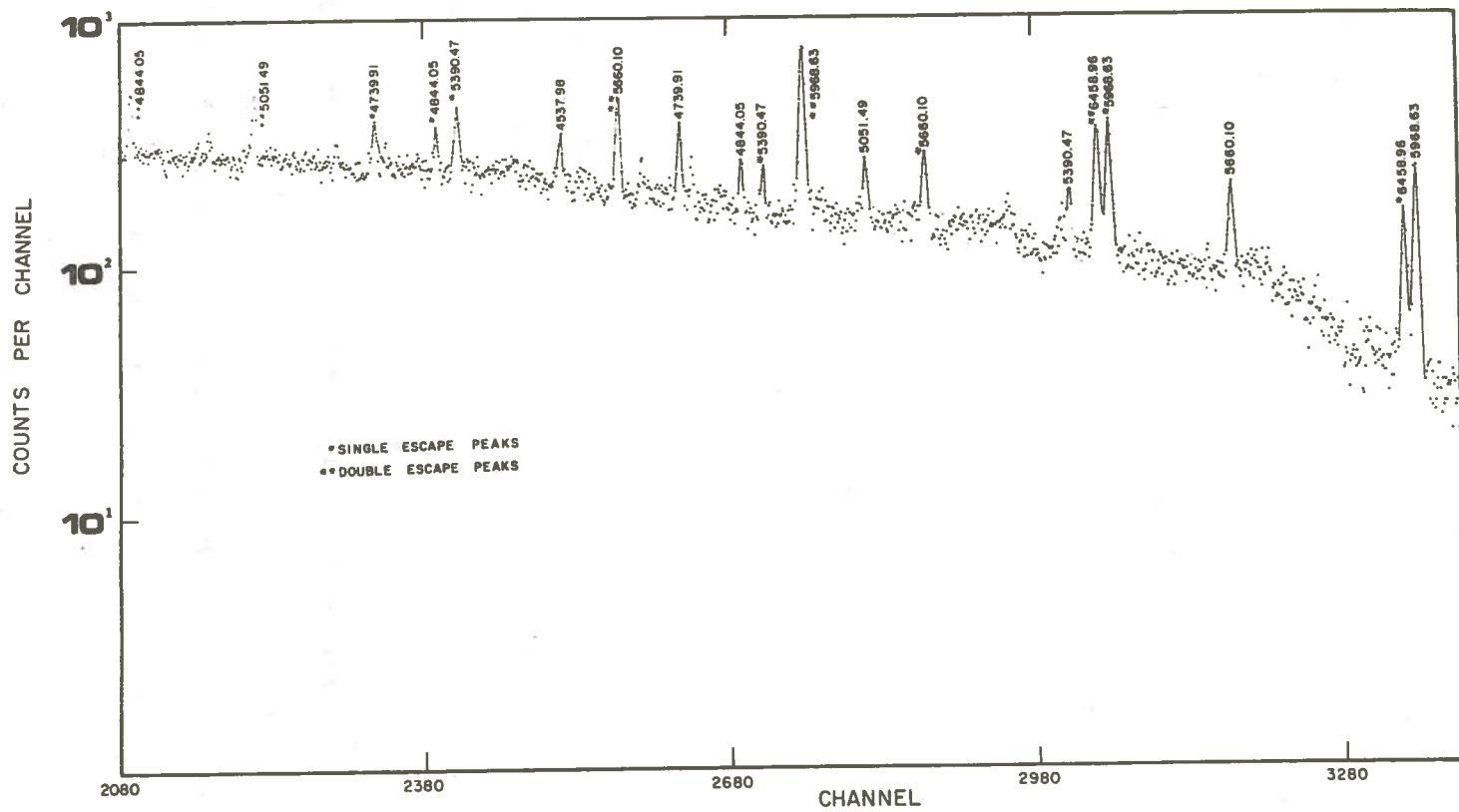


Figure 9(b). The Neutron Capture Gamma-Ray Spectrum From Natural Hg Using a 41 μg ^{252}Cf Source

stronger source in the facility was 2.4 mrem/hr. The observed dose rate was 2.1 mrem/hr as shown in Figure 8(b). Figure 8(b) also shows the dose rates observed at other locations outside the facility.

As mentioned at the beginning of this section the spectroscopic data were obtained using the 3.1 mg ^{252}Cf source. The following were the spectra obtained:

(a) Mercuric oxide spectrum; Figures 10(a) and (b). The amount of HgO used was 9.5 g and the counting time was 8 hr.

(b) Background spectrum; Figure 11. The contributions for this spectrum were from H, B, Al, Pb and the annihilation process. The counting time was 8 hr.

(c) Aluminum spectrum; Figure 12. The target was a cylindrical piece of metallic aluminum having a diameter of 0.375 inch and a length of 1 inch. The counting time was 5-1/2 hr.

(d) Energy calibration spectrum: Figure 13. The contributions for this spectrum were gamma-rays from a standard source¹⁰ which was kept near the detector and gamma-rays from HgO and Al. The counting time was 8 hr.

(e) Carbon tetrachloride spectrum: Figures 14(a) and (b). The amount of CCl_4 used was 3 cm³ and the counting time was 8 hr.

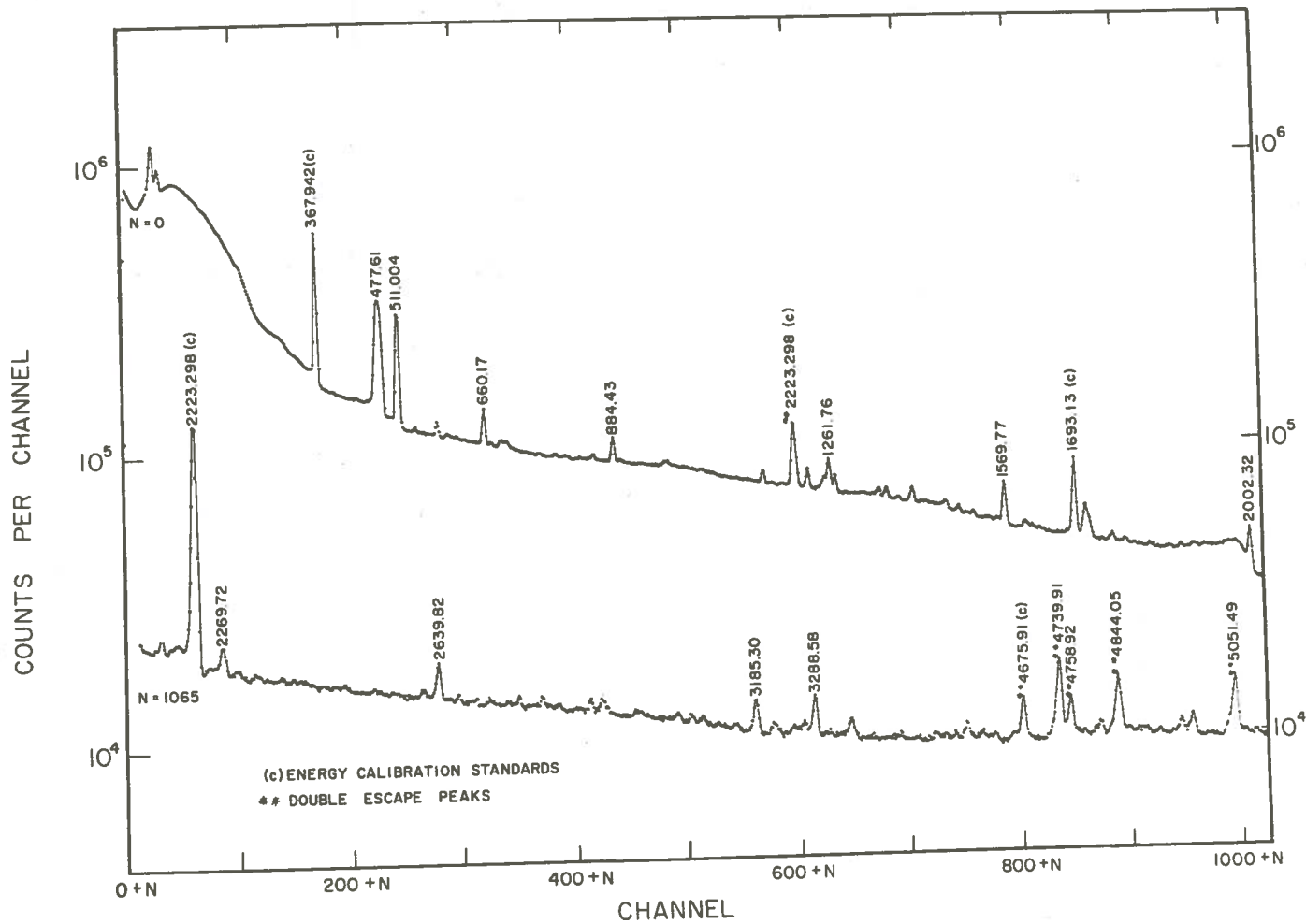


Figure 10(a). The Neutron Capture Gamma-Ray Spectrum From Natural Hg Using a 3.1 mg ^{252}Cf Source

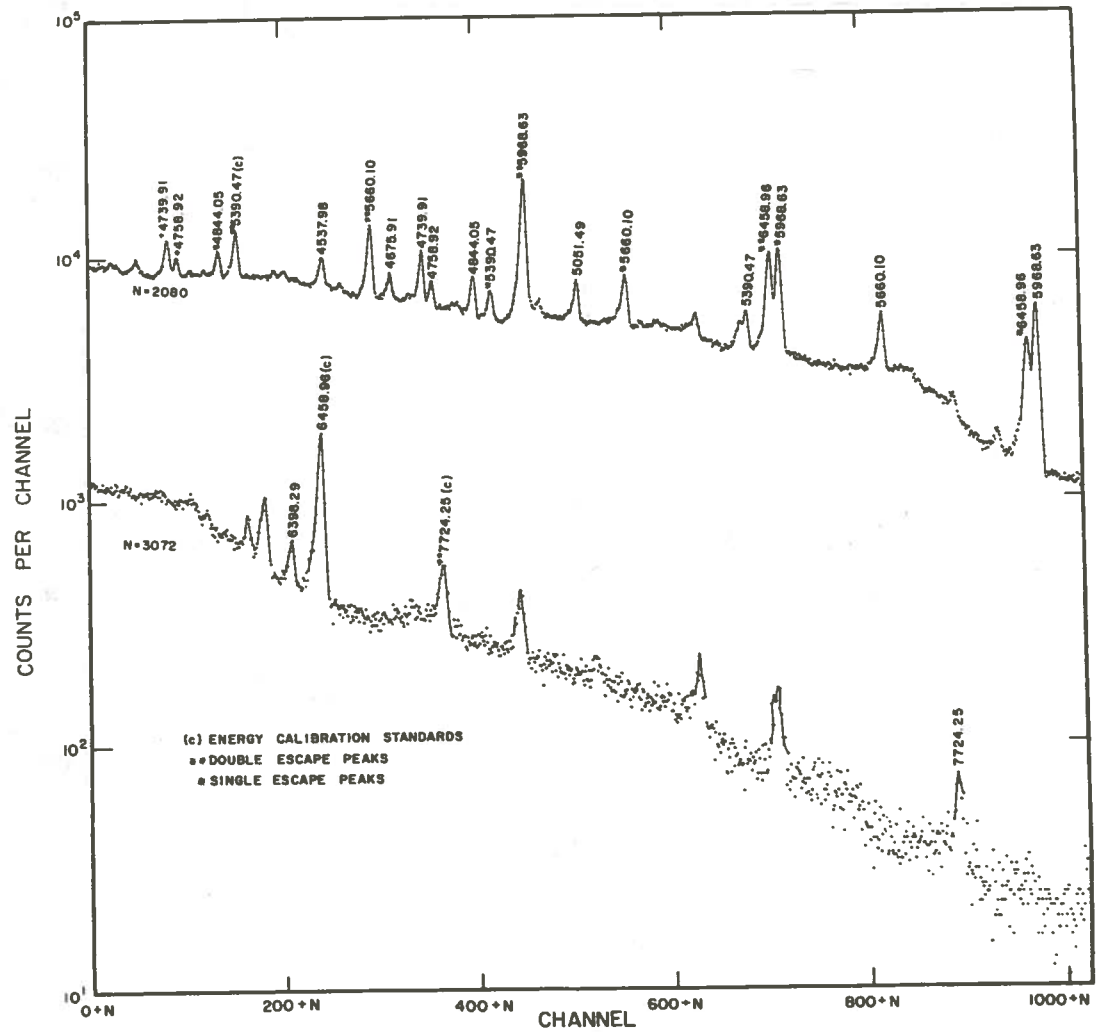


Figure 10(b). The Neutron Capture Gamma-Ray Spectrum From Natural Hg Using a 3.1 mg ^{252}Cf Source

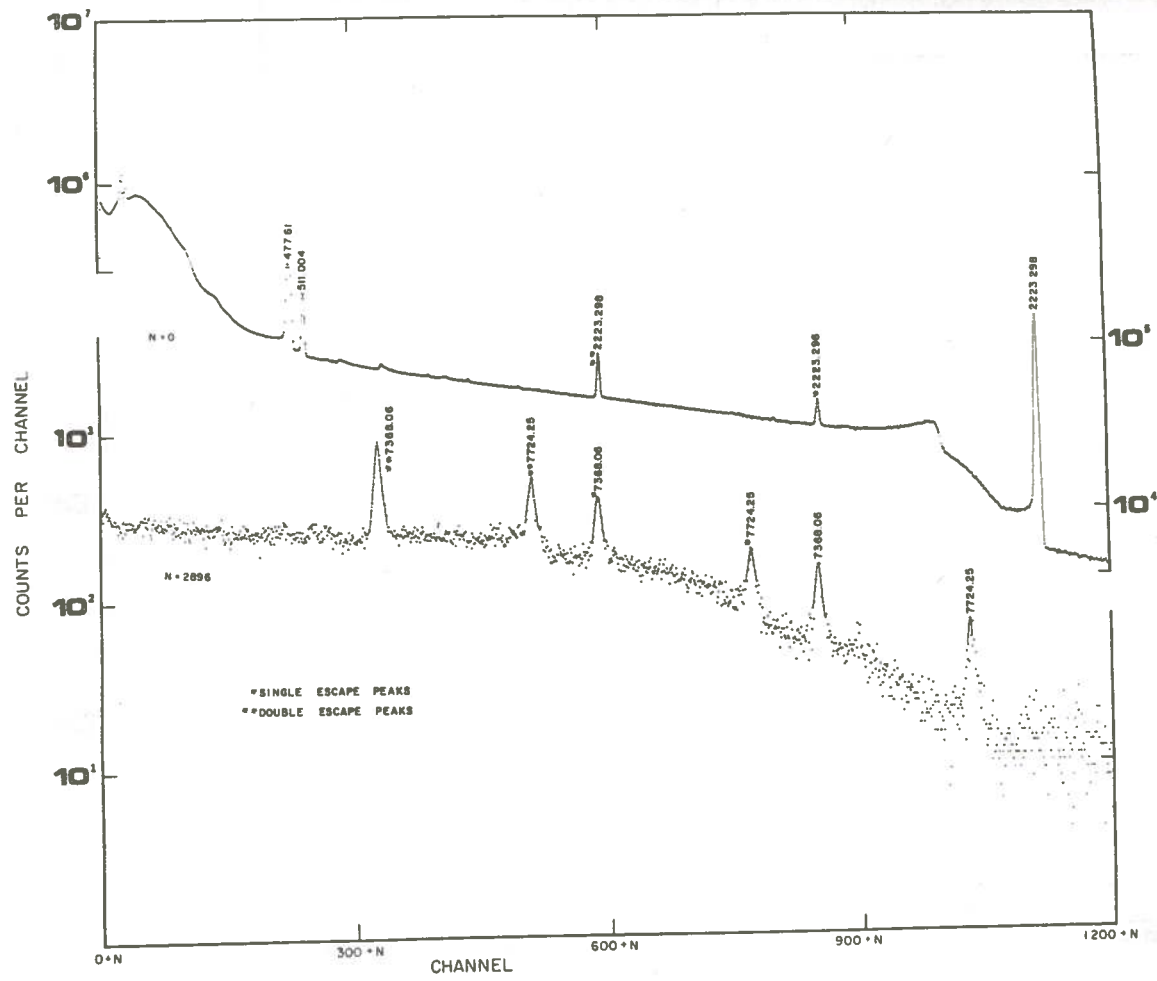


Figure 11. The Background Gamma-ray Spectrum Using a 3.1 mg ^{252}Cf Source

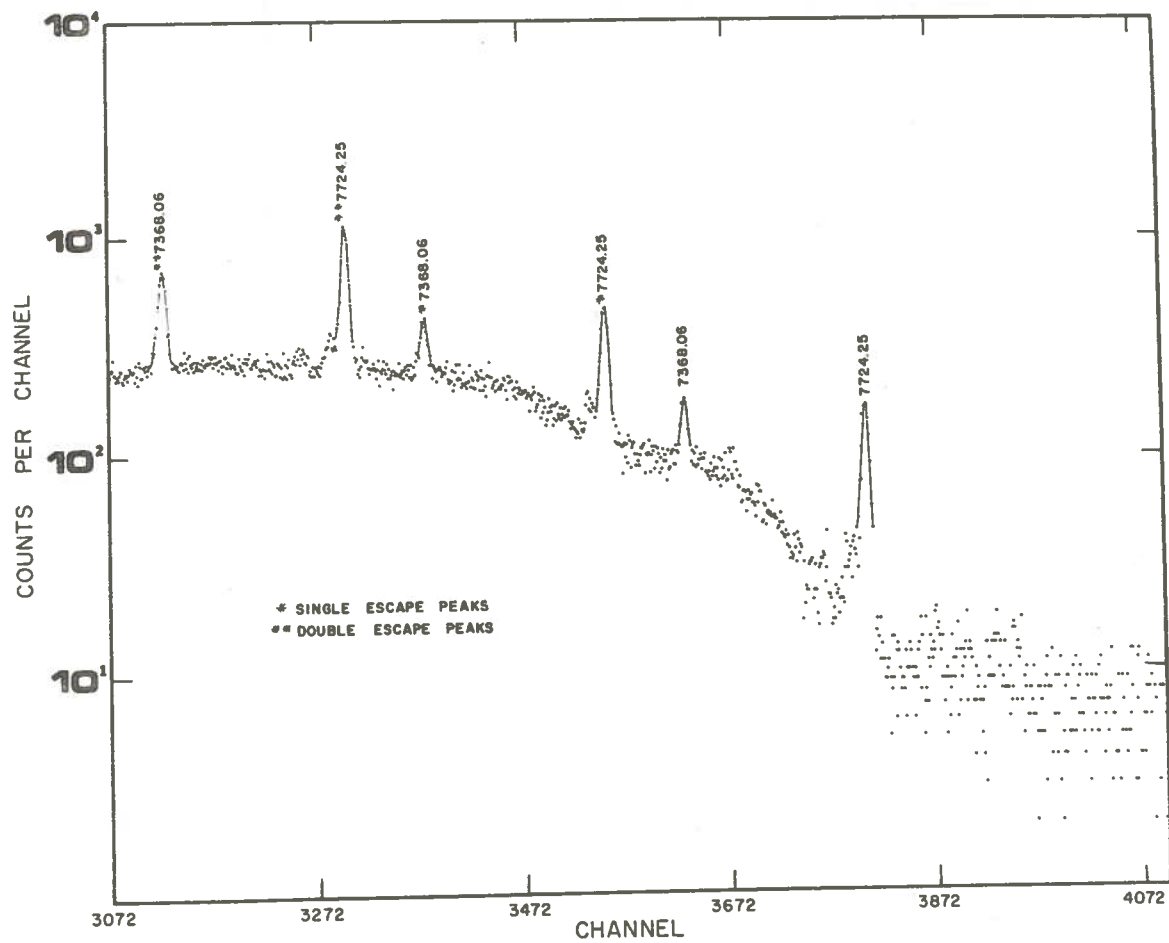


Figure 12. The Neutron Capture Gamma-Ray Spectrum from Al Using a 3.1 mg ^{252}Cf Source

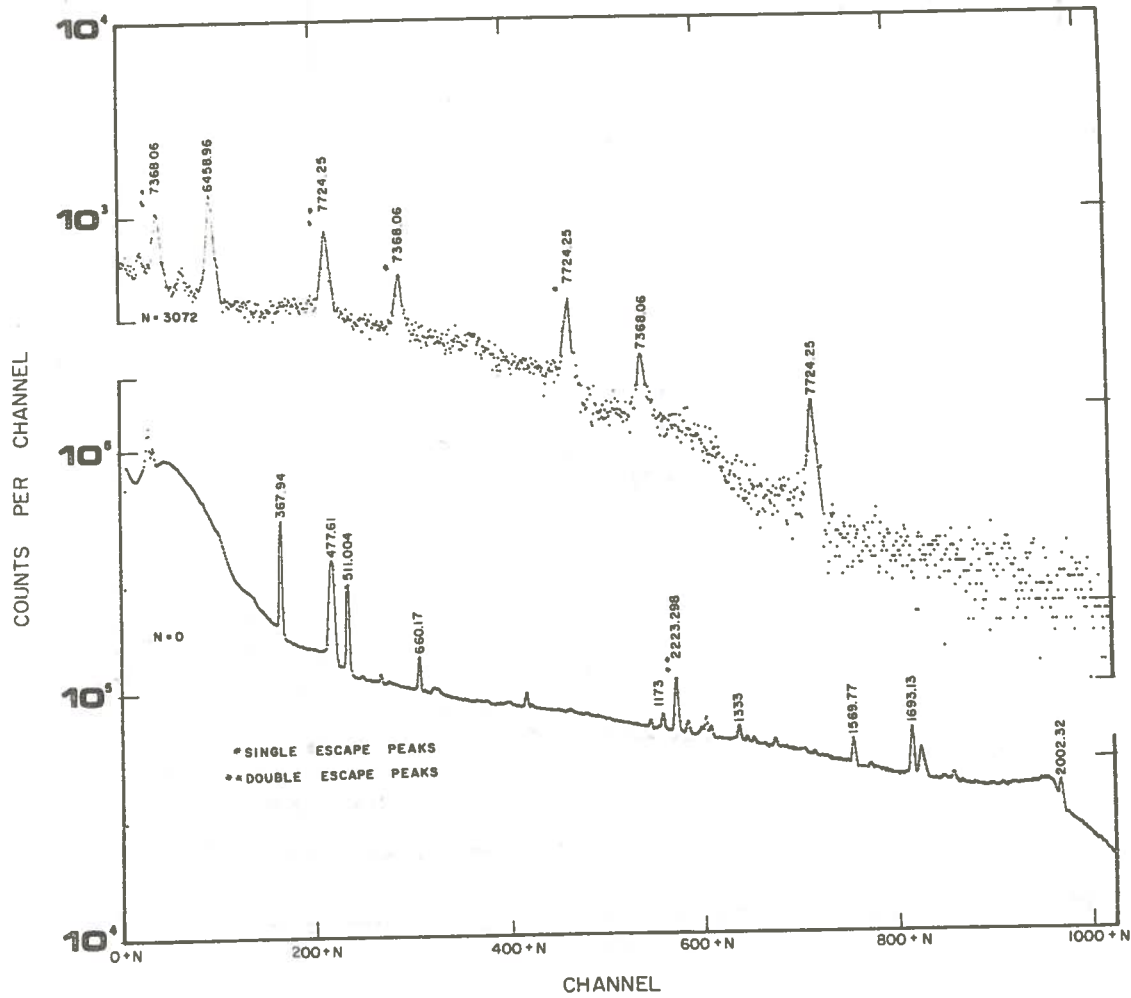


Figure 13. The Energy Calibration Spectrum

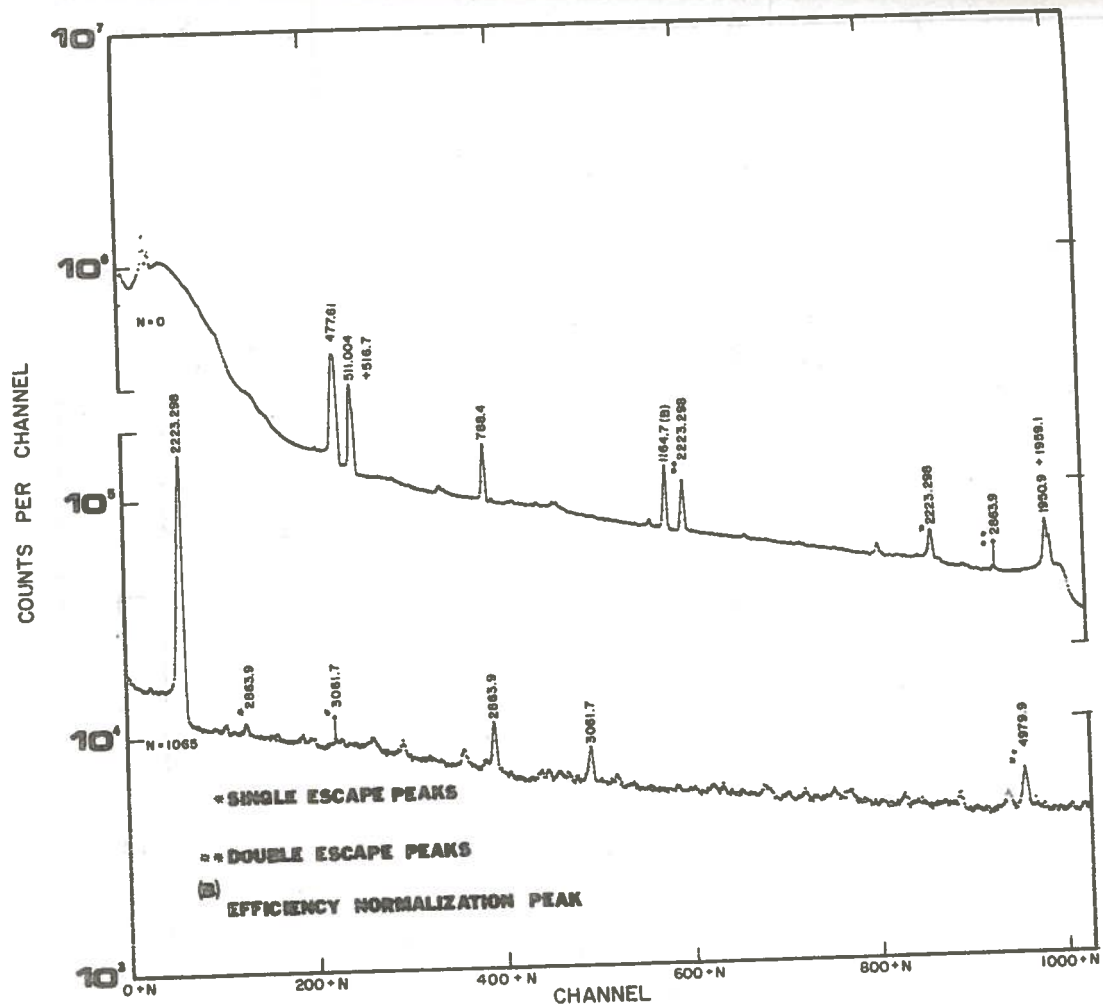


Figure 14(a). The Neutron Capture Gamma-Ray Spectrum from CCl_4 Using a 3.1 mg ^{252}Cf Source.

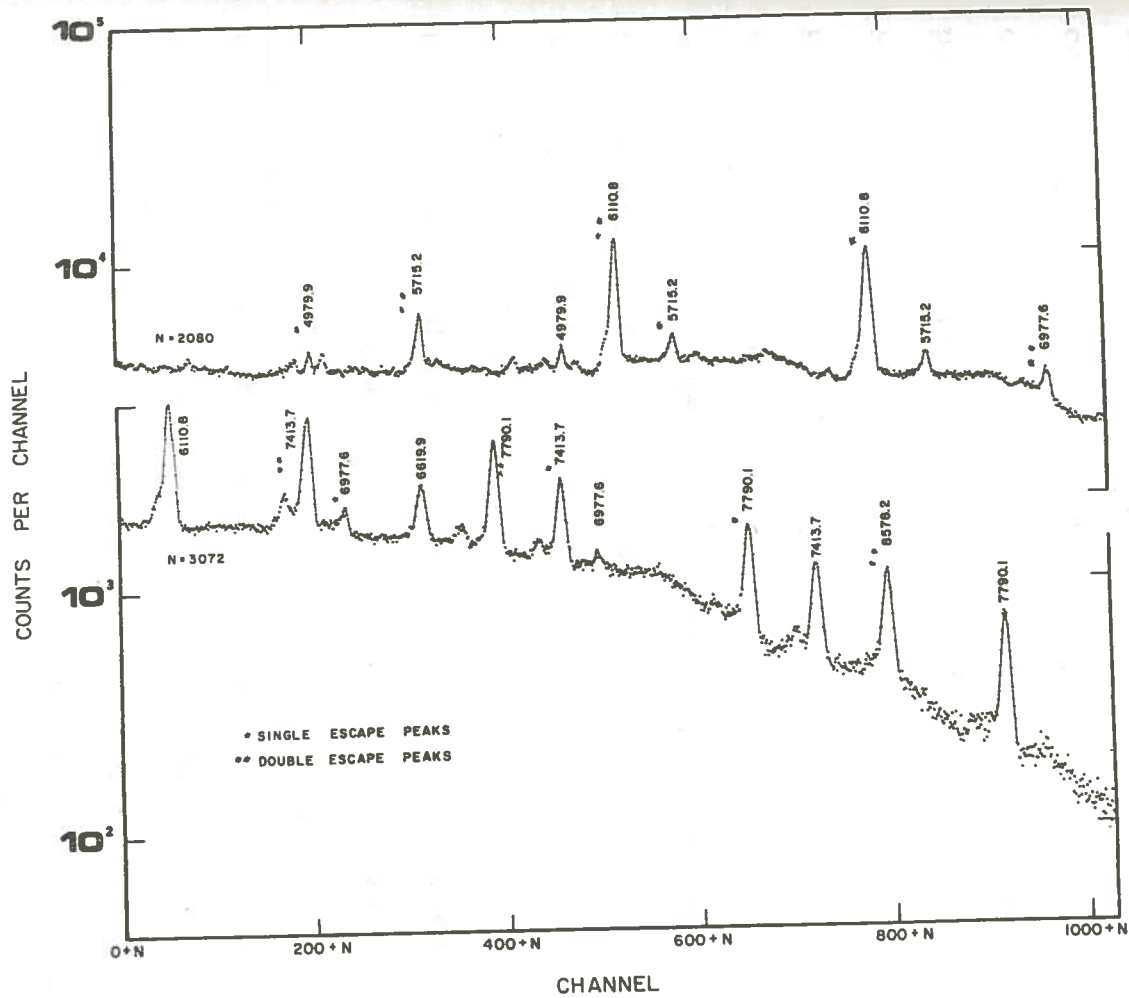


Figure 14(b). The Neutron Capture Gamma-Ray Spectrum from CCl_4 Using a 3.1 mg ^{252}Cf Source

4.4 The Capture Gamma-Ray Spectrum of Natural Hg

In the analysis of a gamma-ray spectrum, the quantities of interest are the energies and the relative intensities of the lines present in the spectrum. Energies can be determined by calibrating the spectrometer. The calibration simply consists of determining two or more parameters necessary to relate the energy corresponding to a photopeak to its channel location in the spectrum. The parameters can be determined using photopeaks corresponding to known gamma-ray energies. Usually a straight line approximation of the form $E = ax + b$, where E is the gamma-ray energy, x is the channel location of the photopeak, "a" is the gain of the analyzer and b is the zero shift of the analyzer is sufficient to determine the energy. The parameters a and b can be determined using energy standards.

The intensities can be determined by evaluating the photopeak efficiency of the detector. The photopeak efficiency $\epsilon_p(E)$ of a detector at an energy E and for a given counting geometry is given by the relation⁸

$$\epsilon_p(E) = N_p / N_o \xi,$$

where N_p is the photopeak counting rate for the gamma-ray of energy E which is emitted from a source with an isotropic emission rate N_o and ξ is the attenuation factor resulting from gamma-ray absorption in the detector housing. A more useful quantity, however, is the relative efficiency $\epsilon_R(E)$ defined by the relation,

$$\epsilon_R(E) = \xi t \epsilon_P(E) = \frac{A}{I} ,$$

where A is the area under the photopeak (total number of counts), I is the relative intensity and t is the counting time. Hence, if the relative efficiency and the area under the photopeak are known at a particular energy, the relative intensity I can be determined. This can be achieved by an efficiency calibration of the detector using photopeak areas and relative intensities of known gamma-rays.

Because of the complexity of the spectrum that was studied, the analysis of data was performed with the use of the computer program SAMPO.¹¹ This program facilitated the determination of the exact channel location of the photopeaks and areas under photopeaks and hence the determination of energies and intensities.

4.4.1 Energy Measurements

The gamma-ray energies were determined using the calibration energies listed in Table 2. These were obtained in the following manner:

The comparison of the energy calibration spectrum with other spectra except that from CCl_4 revealed the presence of the 1173 keV and the 1333 keV lines from the nuclide ^{60}Co which was present in a standard source.¹⁰ Using these two lines the double escape peak (1201.290 keV)

of the hydrogen line (2223.298 keV)¹² was identified. This was observed to be present in the mercury spectrum as well. Using this and the full energy line the intense 1693.13 keV¹³ line from the $^{199}\text{Hg}(n,\gamma)^{200}\text{Hg}$ reaction was identified. By comparing the mercury spectrum with the background spectrum the first intense peak of the mercury spectrum was identified as that due to the 367.942 keV¹³ line from the $^{199}\text{Hg}(n,\gamma)^{200}\text{Hg}$ reaction. This reaction was studied by Breitig et al.,¹³ and the 367.942 keV transition was found to be the most intense. There was no ambiguity in identifying this line. Using this line and the 1201.290 keV line the 511.004 keV¹⁶ line due to annihilation process was identified. The energy values 3653.90 keV, 4368.46 keV, 5660.19 keV and 6458.96 keV were determined using the 2223.298 keV line and the 6702.24 keV line, which is the double escape peak of the 7724.25 keV⁴ line of aluminum. The comparison of the gamma-ray spectrum from aluminum with other spectra enabled one to identify this double escape peak. The lines at these energies were from the reaction $^{199}\text{Hg}(n,\gamma)^{200}\text{Hg}$ as revealed by their agreement with the results of Schult et al.,¹⁴ and Lone et al.¹⁵

TABLE 2

Energy (keV)	Uncertainty (keV)	Reference
367.942	0.010	13
511.004	0.002	16
1201.290 ^d	0.030	12
1693.13	0.14	13
2223.298	0.030	12
3653.90 ^d	1.06	
4368.46 ^d	1.08	
5660.19	1.06	
6458.96	1.06	
6702.24 ^d	0.65	4

^dDouble escape peak energy

4.4.2 Intensity Measurements



The intensities of gamma-rays were determined using the relative efficiency calibration of the detector. The data used to determine this efficiency calibration are listed in Table 3 and the final efficiency curve for the detector for the experimental geometry is shown in Figure 15.

The efficiency calibration was performed in three stages. First, the calibration was performed in the energy range of 367.9 keV to 2639.8 keV using photopeaks due to gamma-rays from ^{200}Hg . The intensities of these transitions were taken from Breitig et al.¹³

In the 2nd stage the efficiency was calculated in the energy range of 788.4 keV to 7413.7 keV using photopeaks due to gamma-rays from the reaction $^{35}\text{Cl}(n,\gamma)^{36}\text{Cl}$. The intensities used in this part of the calculation were those reported by Spits et al.¹⁷

In the 3rd stage the results obtained with the chlorine lines were normalized to the results obtained with the mercury lines in order to achieve a consistent efficiency calibration for the whole range of energy of interest. The normalization was done in the following manner: The photopeak corresponding to the 1164.7 keV line from chlorine was observed to be the most intense one in the spectrum from CCl_4 , lying within the energy range of the mercury lines used in the efficiency calibration in

TABLE 3

Energy (keV)	Source	Relative Efficiency $\epsilon_R(E)$ (Sec)	Relative Efficiency Uncertainty (Sec)
367.9	^{200}Hg	9.75×10^2	40
540.6		1.28×10^3	180
660.1		1.40×10^3	140
884.4		1.28×10^3	130
1146.0		1.21×10^3	180
1407.4		9.44×10^2	120
1693.1		8.42×10^2	110
2002.3		6.21×10^2	90
2639.8	^{200}Hg	5.85×10^2	70
3061.7	^{36}Cl	4.2×10^2	70
4979.9		3.0×10^2	50
5715.2		2.1×10^2	30
6110.8		2.9×10^2	30
7413.7		^{36}Cl	1.7×10^2

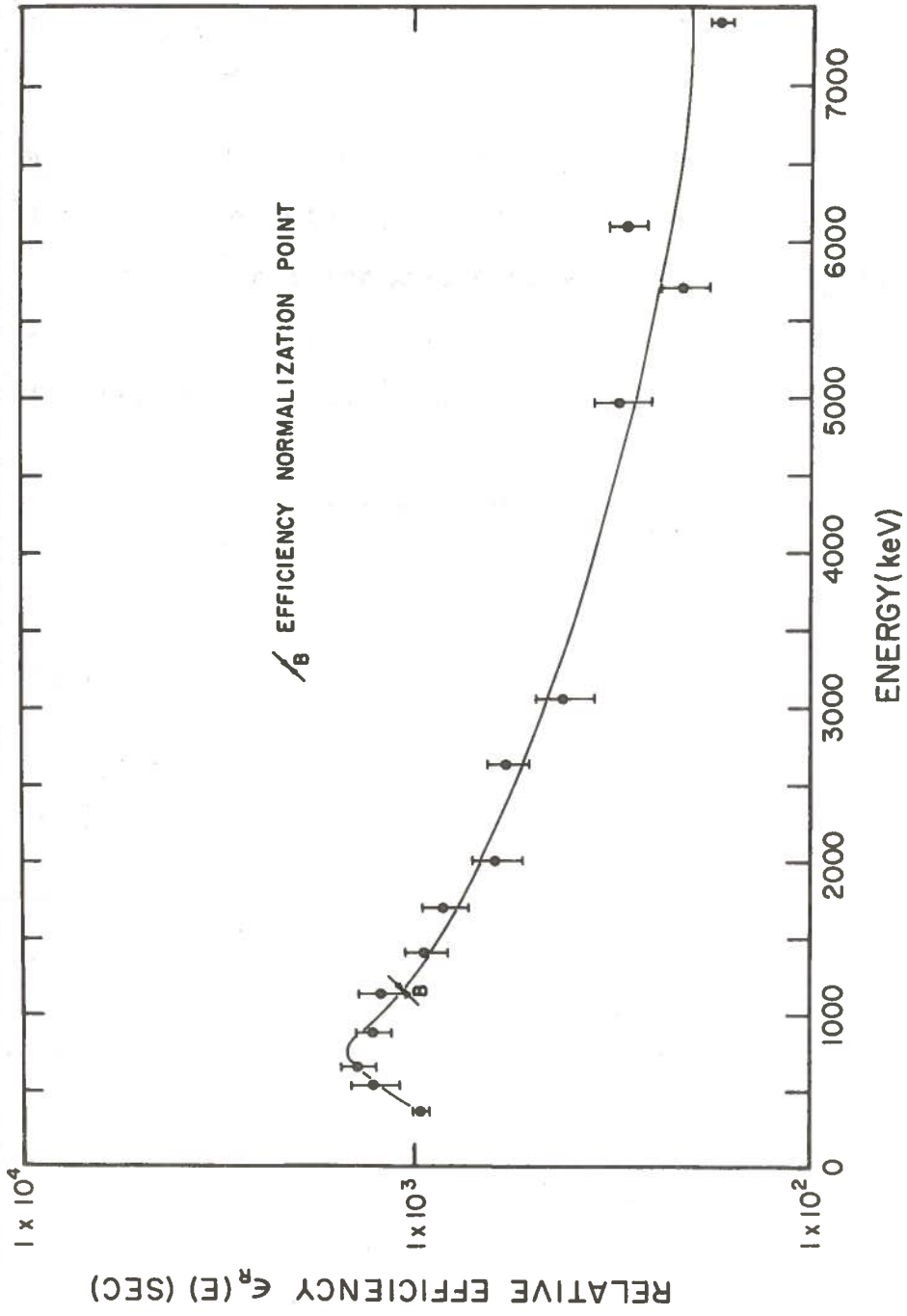


Figure 15. The Photopeak Efficiency Curve for the Detector System

the 1st stage. The efficiency at this energy was compared with the value indicated by the calibration obtained using the mercury lines. The comparison revealed that the values obtained using the chlorine lines had to be scaled down by a factor of 7.2 in order for them to be consistent with those obtained using the mercury lines. The data in Table 3 were obtained after this normalization.

Apart from the relative efficiency calibration, chlorine lines were also used to obtain the variation of $1E/FE$ and $2E/FE$ with full energy E , where

$$\frac{1E}{FE} = \frac{\text{area of the single escape peak}}{\text{area of the full energy peak}}$$

and

$$\frac{2E}{FE} = \frac{\text{area of the double escape peak}}{\text{area of the full energy peak}} .$$

The curves are shown in Figure 16 and the data are listed in Table 4. These curves enable one to determine the areas of the full energy peaks which were not distinct in the spectrum by using the areas of the escape peaks.

TABLE 4

Energy ^{a)} (keV)	1E/FE	2E/FE
7790.1	2.21 ± 0.07	5.11 ± 0.12
7413.7	1.88 ± 0.06	4.35 ± 0.11
6977.6	2.38 ± 0.35	4.61 ± 0.54
6110.8	1.79 ± 0.03	
5715.2	1.22 ± 0.06	2.86 ± 0.11
4979.9	0.88 ± 0.08	1.66 ± 0.11
3061.7	0.19 ± 0.03	
2863.9		0.47 ± 0.03

a) These energies were taken from the work of Spits et al.¹⁷
The photopeaks at these energies were observed in the
gamma-ray spectrum from CCl₄.

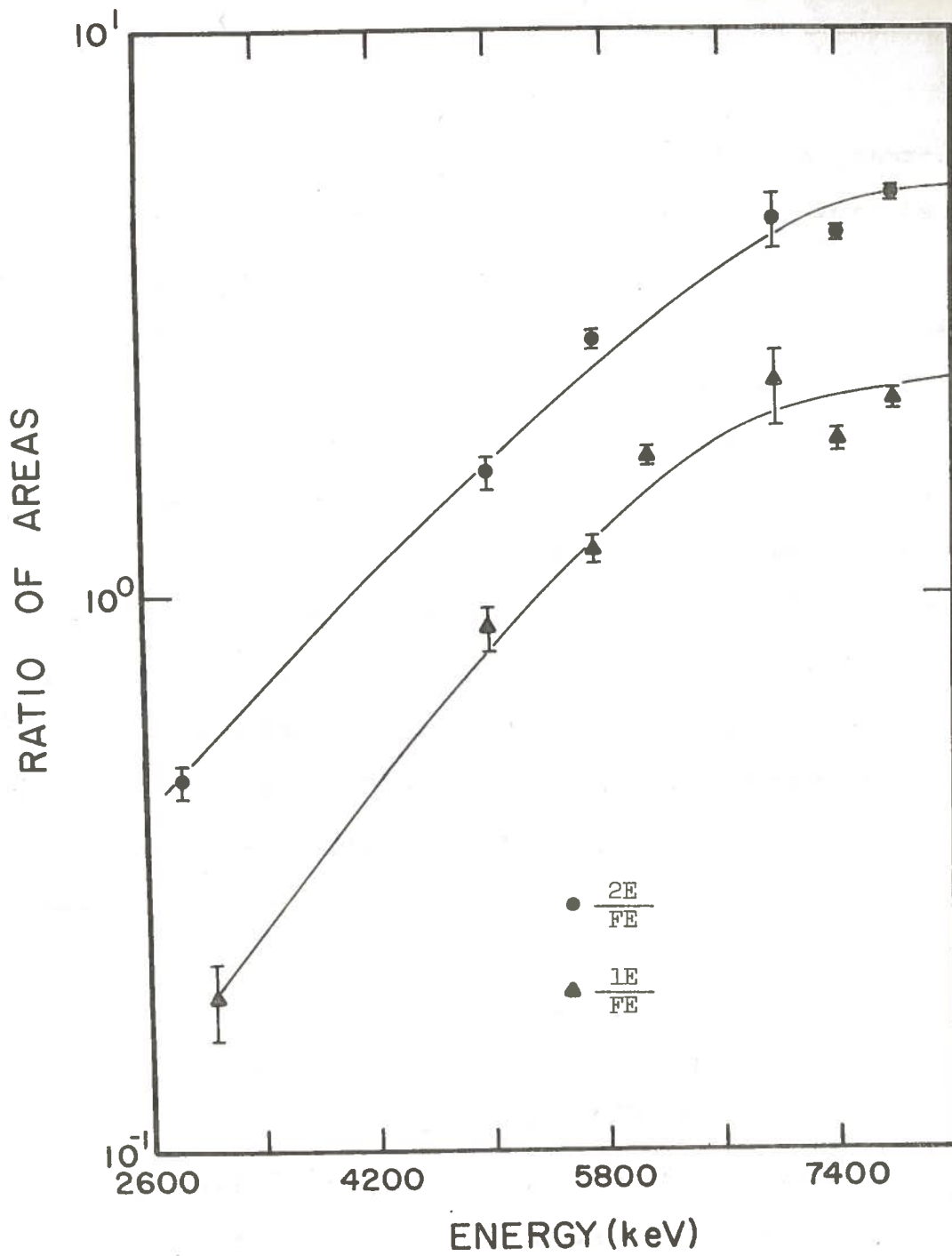


Figure 16. The $1E/FE$ and $2E/FE$ against Full Energy Curves for the Detector System

CHAPTER 5

EXPERIMENTAL RESULTS FROM NEUTRON CAPTURE IN NATURAL Hg

5.1 Isotopic Analysis

After removing the background components, 78 gamma-rays were assigned to the mercury isotopes. The results were then compared with those of Breitig et al.,¹³ Schult et al.,¹⁴ Lone et al.,¹⁵ and Zganjar.¹² In all these experiments reactors were the source of neutrons. Breitig et al.¹³ studied the $^{199}\text{Hg}(n,\gamma)^{200}\text{Hg}$ reaction using a sample of HgS with an isotopic enrichment of 97% in ^{199}Hg . Schult et al.,¹⁴ studied the same reaction using HgO with an isotopic enrichment of 83.45% in ^{199}Hg . Lone et al.¹⁵ studied the resonance neutron capture in $^{198,199,201}\text{Hg}$ using liquid Hg and HgO of natural isotopic composition. Zganjar¹² studied the gamma-ray spectrum from a sample of ^{196}HgO with an isotopic enrichment of 48% in ^{196}Hg .

The comparison of the results obtained in this experiment with the results of the above authors revealed that 72 gamma-rays could be assigned to the reaction $^{199}\text{Hg}(n,\gamma)^{200}\text{Hg}$, 5 to the reaction $^{201}\text{Hg}(n,\gamma)^{202}\text{Hg}$ and 1 to the reaction $^{196}\text{Hg}(n,\gamma)^{197}\text{Hg}$. The results obtained in this experiment together with the results of the above authors are listed in Tables 5, 6 and 7.

TABLE 5
Reaction $^{199}\text{Hg}(n, \gamma)^{200}\text{Hg}$

Results from this work			Energies from Breitig <u>et al.</u> ¹³
Energy (keV)	Rel. Int.* (Decay/Sec)	Rel. Int. Uncertainty Percent (Decay/Sec)	(Thermal neutrons) (keV)
367.942±0.010 ^{e,c,i}	100	6	367.942±0.010
397.73 ±0.36	0.36	18.46	397.765±0.014
438.77 ±0.63	0.43	34.90	439.52 ±0.04
540.67 ±0.21 ⁱ	0.84	12.35	540.948±0.016
578.70 ±0.09	2.58	9.42	579.300±0.017
597.57 ±0.37	0.79	13.54	597.41 ±0.04
611.54 ±0.60	0.49	17.85	612.12 ±0.03
660.17 ±0.08 ⁱ	6.78	9.02	661.36 ±0.03
756.79 ±0.53	0.30	17.17	757.01 ±0.06
784.05 ±0.34	0.43	12.34	783.71 ±0.04
801.95 ±0.51	0.36	17.94	799.90 ±0.18
827.58 ±0.65	0.20	21.57	828.27 ±0.04

TABLE 5 (cont'd)

Results from this work			Energies from Breitig <u>et al.</u> ¹³
Energy (keV)	Rel. Int.* (Decay/Sec)	Rel. Int. Uncertainty Percent (Decay/Sec)	(Thermal neutrons) (keV)
849.36±0.18	0.86	9.48	851.36±0.04
884.43±0.11 ⁱ	3.77	9.06	886.20±0.04
976.97±0.40	0.81	11.92	975.15±0.07
1040.63±0.40	0.31	22.81	1042.4 ±0.3
1146.05±0.17 ⁱ	1.96	10.70	1147.20±0.08
1180.09±1.56	0.28	45.74	1180.4 ±0.4
1224.62±0.13	3.54	10.72	1225.44±0.08
1261.76±0.28	5.19	15.89	1262.96±0.08
1273.06±0.49	2.53	24.45	1273.43±0.10
1348.67±0.18	1.47	8.75	1350.4 ±0.2
1362.40±0.15	1.80	8.30	1363.2 ±0.2
1383.59±0.39	0.67	12.52	1385.0 ±0.3

TABLE 5 (cont'd)

Results from this work			Energies from Breitig <u>et al.</u> ¹³
Energy (keV)	Rel. Int.* (Decay/Sec)	Rel. Int. Uncertainty Percent (Decay/Sec)	(Thermal neutrons) (keV)
1407.41±0.11 ⁱ	2.59	6.77	1408.0 ±0.2
1465.68±0.27	1.25	8.07	1467.6 ±0.3
1488.84±0.29	0.93	9.85	1488.5 ±0.4
1514.35±0.39	0.69	11.77	1514.8 ±0.3
1569.77±0.13	7.53	5.64	1570.45±0.15
1605.93±0.25	1.04	8.13	1604.5 ±0.2
1693.13±0.14 ^{e,c,i}	14	6	1693.13±0.14
1758.86±0.22	1.09	7.31	1759.3 ±0.3
1781.06±0.35	0.61	10.33	1783.3 ±1.0
1825.26±0.62	0.39	17.38	1825.9 ±0.5
1858.76±0.65	0.29	17.50	1857.4
1921.82±0.56	0.39	14.39	1921.1 ±0.3
2002.32±0.16 ⁱ	5.56	6.69	2002.1 ±0.2

TABLE 5 (cont'd)

Energy (keV)	Results from this work		Energies from Breitig <u>et al.</u> ¹³
	Rel. Int.* (Decay/Sec)	Rel. Int. Uncertainty Percent (Decay/Sec)	(Thermal neutrons) (keV)
2269.72±0.89	3.05	17.85	2271.5±0.4
2295.04±3.36	0.85	57.50	2296.3±0.3
2370.45±0.49	0.36	13.85	2370.0±0.3
2479.51±0.46	0.33	11.09	2480.2±1.5
2529.39±0.60	0.26	15.32	2528.7±0.4
2639.82±0.34 ⁱ	2.90	6.29	2639.9±0.2
2727.67±0.41	0.45	13.64	2727.2±0.3
2846.35±0.69	0.32	14.55	2847.3±0.6
2901.04±0.60	0.81	10.94	2901.3±0.3
2921.56±0.59	1.18	8.77	2921.1±0.3
3050.63±0.72	0.54	9.51	3051.1±0.8
3074.52±0.70	0.57	9.65	3074.2±0.6

TABLE 5 (cont'd)

Results from this work			Energies from Breitig <u>et al.</u> ¹³
Energy (keV)	Rel. Int.* (Decay/Sec)	Rel. Int. Uncertainty Percent (Decay/Sec)	(Thermal neutrons) (keV)
3185.30±0.73	2.64	5.88	3185.8 ±0.4
3217.28±0.85	0.80	9.35	3216.9 ±0.8
3269.54±0.98	0.57	17.19	3269.4 ±0.6
3288.58±0.81	2.95	6.25	3288.9 ±0.4
			Energies from <u>Schult et al.</u> ¹⁴
			(Thermal neutrons)
3351.68±0.87	1.39	6.18	3352.8 ±1.5
4459.98±1.05	0.36	21.06	4458.8 ±1.5
4537.98±1.30	2.25	30.71	4537.8 ±1.5
4555.68±1.20	0.23	30.97	4555.5 ±1.5
4675.91±1.07 ^d	3.13	9.18	4675.52±0.50

TABLE 5 (cont'd)

Energy (keV)	Results from this work		Energies from Schult <u>et al.</u> ¹⁴
	Rel. Int.* (Decay/Sec)	Rel. Int. Uncertainty Percent (Decay/Sec)	(Thermal neutrons) (keV)
4739.91±1.08	8.07	6.55	4739.22±0.40
4758.92±1.09	3.73	8.86	4758.92±0.40
4811.71±1.07	0.82	17.95	4811.77±0.50
4844.05±1.07	5.00	6.58	4842.44±0.35
4955.35±1.15	1.78	14.23	4954.17±0.50
4975.61±1.17	1.36	12.22	4974.67±0.45
5051.49±1.07	5.42	6.10	5050.32±0.40
5390.47±1.07 ^d	4.08	6.31	5388.74±0.35
5660.19±1.06 ^c	6.09	6.34	5658.74±0.40
5968.63±1.06	14.6	6.5	5967.47±0.20
6310.82±1.17	0.68	11.42	6310.27±0.30
6398.29±1.08	0.82	7.50	6397.74±0.20
6458.96±1.06	5.49	7.04	6458.42

TABLE 5 (cont'd)

* The relative intensities are normalized to the results of Breitig et al.¹³

c) These energies were used in the energy calibration.

d) Double escape peak energy values of these were used in the energy calibration.

i) These were used in the efficiency calibration.

e) These energies were borrowed from Breitig et al.¹³

TABLE 6
 Reaction $^{201}\text{Hg}(n, \gamma)^{202}\text{Hg}$

Results from this work			Energies from Lone <u>et al.</u> ¹⁵
Energy (keV)	Rel. Int.* (Decay/Sec)	Rel. Int. Uncertainty Percent (Decay/Sec)	(Resonance neutrons; 43, 70.9, 210.3 eV): (keV)
4274.97±1.47	0.39	23.56	4275.0 ±2.5
4404.42±1.11	0.65	23.19	4405.3 ±1.2
4577.09±1.20	0.85	12.22	4576.5 ±2.6
4804.01±2.06	0.37	50.62	4805.0 ±1.8
6230.21±1.39	0.29	20.29	6231.4 ±1.1

*The relative intensities are consistent with the normalization of the values listed in Table 5.

TABLE 7
 Reaction $^{196}\text{Hg}(n,\gamma)^{197}\text{Hg}$

Results from this work			Energies from Zganjar ¹²
Energy (keV)	Rel. Int.* (Decay/Sec)	Rel. Int. Uncertainty Percent (Decay/Sec)	(Thermal neutrons) (keV)
4521.65±1.07	0.48	18.55	4522.38±0.64

* The relative intensity is consistent with the normalization of the values listed in Table 5.

5.2 Decay Scheme for ^{200}Hg

When a neutron is captured by a nucleus of mass number A the result is the formation of another nucleus of mass number $A+1$, in a highly excited state. The nucleus formed is referred to as the compound nucleus and the initially excited state is referred to as the capture state. The process can schematically be represented by the equation:

$$M_A + M_n = M_{A+1} + Q ,$$

where M_A is the mass of the target nucleus, M_{A+1} is the mass of the compound nucleus and M_n is the mass of the neutron. The energy balance in the reaction, Q , which is the binding energy of the last neutron in the compound nucleus plus the kinetic energy of the incident neutron is shared between the many nucleons in the compound nucleus and it is left in a highly excited state. In thermal neutron capture the excitation energy is typically of the order of 8 MeV. The thermal neutrons are s-wave neutrons and the capture of these neutrons by a target nucleus with spin and parity I_t, π_t leads to the excitation of a capture state with spin and parity $I_c, \pi_c = I_t \pm 1/2, \pi_t$. In this way $I_c = 1/2$, states are produced from even-even target nuclei, because the target spin is 0 and $I_c = I_t \pm 1/2$ states are produced from odd target nuclei. In the latter case

both states contribute in general to the capture process. In gamma decay the excitation energy is carried off in one or more radiative transitions to nuclear states at lower energies. The known nuclei have low spins and hence, low-spin states are preferentially populated through the (n, γ) reaction which are very useful in the study of nuclear structure at low spin. The energy E_γ , of the gamma-ray emitted when a level of energy E_1 de-excites to a lower level of energy E_2 is given by

$$E_\gamma = E - \frac{E_\gamma^2}{2M_{A+1}c^2},$$

where $E = E_1 - E_2$ is the level separation energy, M_{A+1} is the mass of the nucleus and $E_\gamma^2/2M_{A+1}c^2$ is the recoil energy of the nucleus. Hence, knowing the gamma-ray energies, the energies of the nuclear levels can be determined with the ground state at an energy of zero and the decay scheme can be developed.

Figure 17 shows the decay scheme developed for the nucleus ^{200}Hg , in this work. Because we were dealing with a heavy nucleus, the calculated recoil energies were smaller than the uncertainties in the gamma-ray energies and were not considered. The neutron separation energy for ^{200}Hg is 8028.8 ± 0.5 keV,^{4,13} hence it was taken as the energy of the capture state. The spins and parities were taken from Breitig et al.,¹³ Schult et al.,¹⁴ and Martin.¹⁸

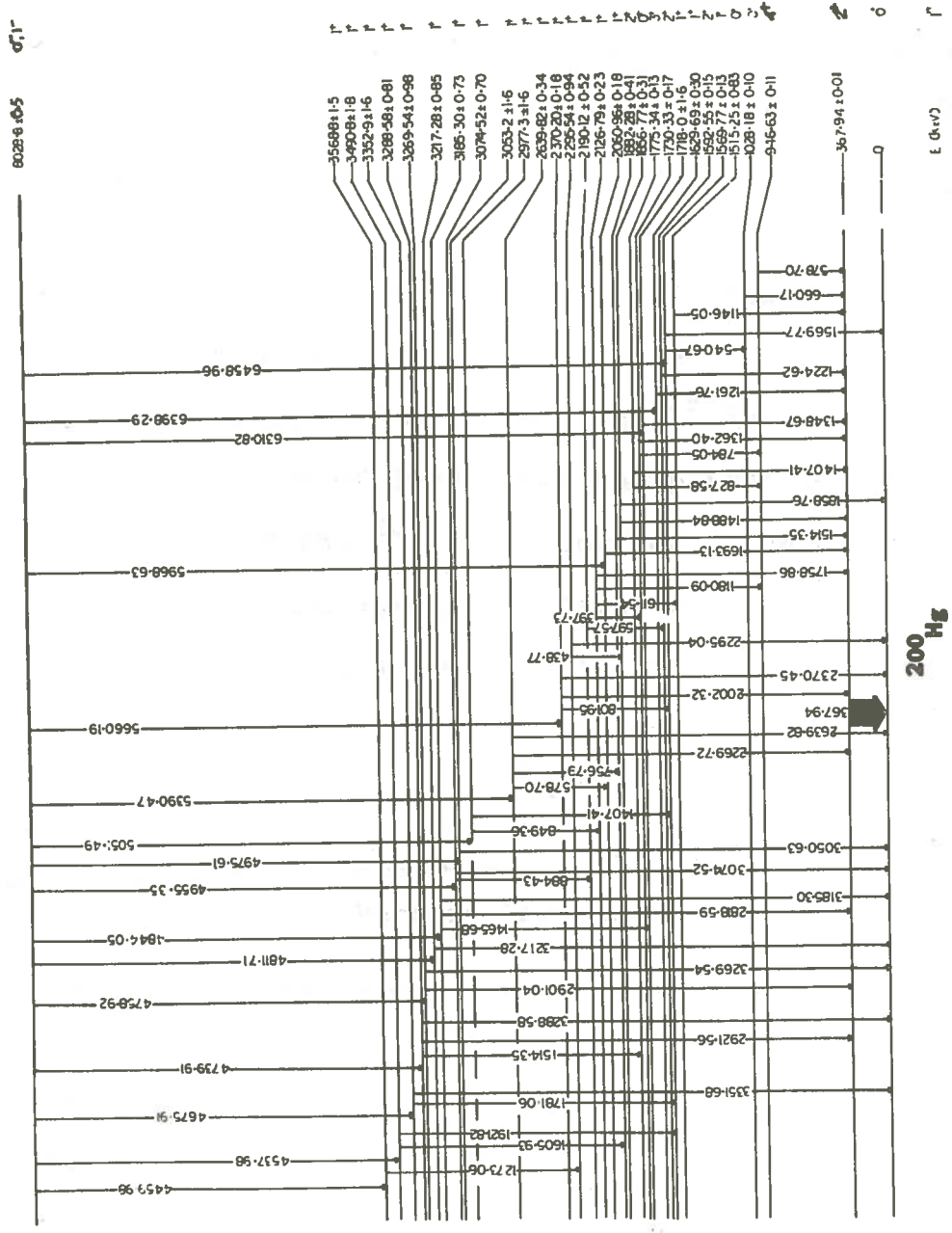


Figure 17. The Decay Scheme for ^{200}Hg

CHAPTER 6
DISCUSSION

Altogether 78 gamma-rays were observed from neutron capture in mercury where 92% of the observed transitions belonged to the $^{199}\text{Hg}(n,\gamma)^{200}\text{Hg}$ reaction. The reason for this is evident from a study of the thermal neutron capture cross sections and the percentage abundance of the mercury isotopes which are listed in Table 8.⁴ The ^{199}Hg isotope has a thermal neutron capture cross section of 2000b and a percentage abundance of 16.9. The ^{196}Hg isotope has a high cross section of 3080b, but the percentage abundance is only 0.15 and the ^{201}Hg isotope has a low cross section of 60b. Hence, the dominant character of ^{200}Hg γ -rays from capture in natural mercury is inevitable.

TABLE 8

Isotope	Percent Abundance	Thermal Cross Section
^{199}Hg	16.9	2000b
^{201}Hg	13.2	60b
^{196}Hg	0.5	3080b

Altogether 28 excited levels were deduced for ^{200}Hg . Sixty-three of the seventy-two observed transitions were placed in a level scheme. The difficulty in placing the

other nine transitions could be attributed to the fact that the levels associated with these transitions might have been populated weakly and the data is insufficient to reveal their existence. The levels deduced in this experiment were found to be in agreement with the levels reported by Breitig et al.,¹³ Schult et al.,¹⁴ and Martin¹⁸ showing the applicability of the facility to nuclear structure studies.

CHAPTER 7

CONCLUSIONS

The results from thermal neutron capture in mercury show that the facility can be utilized successfully in nuclear energy level studies and in isotopic analysis over a wide range of cross sections, from 60b to 3080b and over a wide range of isotopic abundance, from 0.15% to 16.9%. The observation of gamma-rays from aluminum indicates that the facility can be used in thermal neutron capture gamma-ray spectroscopy with target materials having cross sections as low as 230 mb,⁴ even though the spectrum from aluminum was not subjected to detailed analysis. The facility will work exceptionally well in isotopic analysis since one needs much less sensitivity in that application than for level scheme studies. The identification of one gamma-ray from each isotope is usually sufficient to accomplish the analysis. Furthermore, the feasibility of the facility in elemental analysis is noteworthy and one can easily identify the strongest element having the highest thermal cross section and abundance from the study of the capture gamma-ray spectrum.

LIST OF REFERENCES

1. R. C. Greenwood, CONF-720902, Proceedings of the American Nuclear Society (September 1972).
2. Peter F. Wiggins et al., CONF-720902, Proceedings of the American Nuclear Society (September 1972).
3. Du Pont, Report No. 1246, "Californium-252" (1976).
4. BNL 325, Vol. 1, "Neutron Cross Sections".
5. J. J. Fitzgerald, G. L. Brownell and F. J. Mahoney, "Mathematical Theory of Radiation Dosimetry".
6. General Dynamics Corporation, Fort Worth Division, Texas; Californium-252 Progress No. 5 (November 1970).
7. Hans Fiedler and Orren Tench, Germanium (Li) Gamma Spectrometer Systems, Canberra Industries, Inc.
8. George Earl Keller, Ph.D. Dissertation, LSU, Baton Rouge (1969).
9. Du Pont, Report No. 1232, "Californium-252" (1976).
10. NBS, Reference Material 4216-B, "Standard Source".
11. Jorma T. Routti, "SAMPO", LRL, University of California, Berkeley.
12. E. F. Zganjar, private communication, Department of Physics, Louisiana State University, Baton Rouge, La.
13. Breitig et al., Phys. Rev. C, Vol. 9, No. 1 (January 1974).
14. Schult et al., Phys. Rev. , Vol. 164, No. 4 (December 1967).

15. Lone et al., Nuclear Physics A 243 (1975) 413.
16. Hans Frauenfelder and Ernest M. Henley, "Subatomic Physics".
17. Spits et al., RCN, Petten (June 1975).
18. Martin, Nuclear Data Sheets, Vol. 6, No. 4 (1971).